Quantum-classical correspondence in the phase control of multiphoton dissociation by two-color laser pulses

Emanuel F. de Lima* and Marcus A. M. de Aguiar
Instituto de Física Gleb Wataghin, Universidade Estadual de Campinas, Unicamp 13083-970, Campinas São Paulo, Brazil
(Received 26 November 2007; revised manuscript received 8 January 2008; published 10 March 2008)

The quantum and the classical multiphoton dissociation dynamics of diatomic Morse molecules driven by intense and ultrashort two-color laser pulses are investigated and compared. Special attention is given to the role of the relative phase of the monochromatic components of the pulses. We study the excitation of the system from the vibrational ground state and from excited states for several values of amplitude, frequency, and duration of the external pulses. Similar overall sensitivity of the dissociation threshold on the phase is observed in both quantum and classical approaches, provided the excitation frequency is sufficiently far from quantum resonances. In addition, we analyze the correspondence between the effects of the relative phase on the classical and quantum dynamics.

DOI: 10.1103/PhysRevA.77.033406 PACS number(s): 33.80.Wz, 05.45.Mt, 33.80.Rv

I. INTRODUCTION

Quantum-classical correspondence in classically chaotic systems is an important subject in quantum theory [1–7]. In the semiclassical limit, classical mechanics becomes a fundamental tool for the study of microscopic systems, especially when the application of *ab initio* quantum calculations are cumbersome. The fact that the classical dynamics associated to atoms and molecules driven by external fields is, in general, nonintegrable brings up the question as to whether one can relate classical chaos to quantum dynamics, the so-called quantum chaos [8–10]. Furthermore, the advances in quantum control theory [11–18] raise the additional theme of the implications of coherent control in classically chaotic molecular systems [19–21].

The control of atomic and molecular dynamics by two-color laser fields is an issue of considerable current interest [22–25]. It has been experimentally demonstrated that the processes of ionization and dissociation are both sensitive to the relative phase of bichromatic laser fields [26–28]. The phase dependence can be interpreted in terms of interference of the quantum amplitudes of competing excitation pathways [11,13,29,30]. However, there are other ways to picture the phase effects present in ionization and dissociation as, for instance, in relation to the interference between the components of the external field [31,32]. In particular, it has been shown that the classical and quantum calculations agree and reproduce the experimental shifts with respect to the relative phase of the ionization threshold of highly excited hydrogen atoms driven by a two-color microwave field [33]. This striking result allowed an interpretation of the phase dependence of ionization in terms of the classical nonlinear common resonances [33]. Therefore, it is important for the applications of semiclassical methods to determine the existence and extension of quantum-classical correspondence in other atomic and molecular dynamical systems.

In this work, we consider the standard model of the driven Morse oscillator in the nonpertubative regime representing the interaction of a diatomic molecule with laser fields. It has been widely recognized that the laser-driven classical dissociation of the Morse oscillator occurs through chaotic routes [34–38]. For weak fields, the phase space is dominated by Kolmogorov-Arnold-Moser (KAM) tori and the chaotic layers related to unstable periodic orbits of nonlinear resonances cover a relatively small portion of the phase space (local chaos) [39,40]. As the driving increases, the resonance islands grow and eventually overlap each other, whereas most of the KAM tori vanish. The phase-space dynamics then become dominated by chaotic orbits (global chaos) which can lead to dissociation. Such chaotic behavior have motivated numerous quantum-classical correspondence studies, since the Morse model allows for direct comparison of the two theories [41–47]. Here, we extend the previous pure classical investigation of Constatoudis and Nicolaides [48] by comparing the quantum and the classical dependence of the dissociation probability on the relative phase of two-color pulses. Constatoudis and Nicolaides found that the deformation and movement of the KAM tori are mostly responsible for the classical dissociation probability dependence on the relative phase. The central point we address is to whether the effects connected with the phase dependence observed in the classical mechanics are also produced by quantum mechanics. This question is far from obvious since the correspondence observed in the ionization of excited hydrogen atoms by microwave fields [33] is not guaranteed *a priori* in other circumstances. Moreover, it is important for appropriate classical-based interpretations to find out the system parameters for which the correspondence does or does not occur.

Since the molecular control in the ultrafast regime with different frequency combinations are required for many applications of quantum control, pulses in the range of picoseconds with several frequency ratios are considered. We carry out an extensive numerical study of the dissociation dynamics from the ground state and also from excited vibrational levels. It is worth noting that instead of the linear dipole approximation used in Ref. [48], we consider a more realistic form for the dipole interaction function. We solve the quantum equations applying a recently developed technique, which merges the standard basis-state approach with the ex-

*eflima@ifi.unicamp.br; Current address: Department of Chemistry, Princeton University, Princeton, NJ, 08544.

pansion of the continuum coefficients in terms of generalized Laguerre polynomials [49,50]. The advantage of this method compared to the approaches that solve the Schrödinger equation on a grid [51–53] is the straightforward knowledge of the occupation probabilities of the vibrational levels whereas avoiding the artificial introduction of absorbing boundaries. Our calculations show that the dissociation probability can be controlled by manipulating the relative phase of the components of the pulse. Furthermore, we verify that the classical phase effects on the shifts of the dissociation threshold are in good agreement with the quantum ones for a wide range of the system parameters. We also show that the correspondence breaks down when the laser frequency is tuned close to the quantum resonances. Finally, we examine the alterations in the phase-space induced by the relative phase of the pulse and the corresponding changes in the quantum population dynamics.

II. MODELS AND METHODS

We consider the driven Morse oscillator as our model for the investigation of the classical-quantum correspondence. This system can theoretically account for the dissociation of a diatomic molecule by linearly polarized laser fields [53]. More realistic descriptions of the molecular dissociation should include the rotational degrees of freedom and also the possibility of electronic excitation. However, since the focus of the present work is on the relations between the classical and quantum theories, the use of this simpler system is legitimate. The total time-dependent Hamiltonian H can be written in two parts, one representing the free molecule, H_0, and the other the molecule-field interaction, H_1,

$$H(r,p,t) = H_0(r,p) + H_1(r,t), \tag{1}$$

where r is the internuclear distance.

The Hamiltonian $H_0(r,p)$ is given by the free Morse oscillator,

$$H_0(r,p) = \frac{p^2}{2m} + D\{\exp[-2\beta(r-r_e)] - 2\exp[-\beta(r-r_e)]\}, \tag{2}$$

where D is the dissociation energy, β^{-1} is the range of the potential, r_e is the equilibrium position, and m is the reduced mass of the nuclei.

The interaction Hamiltonian $H_1(r,t)$ is given in the semiclassical approximation by

$$H_1(r,t) = -\mu(r)\mathcal{E}(t), \tag{3}$$

where $\mathcal{E}(t)$ represents the electric field component along the molecular dipole.

We write the dipole function $\mu(r)$ as

$$\mu(r) = qr\exp(-r/r_d), \tag{4}$$

where q is the effective charge and r_d gives the range of the interaction.

The external field is given by a two-color pulse composed by the carrier frequencies ω and $\alpha\omega$,

$$\mathcal{E}(t) = f(t)[\cos(\omega t) + \xi\cos(\alpha\omega t + \phi)], \tag{5}$$

where ξ and α give, respectively, the ratio between the amplitudes and frequencies of the pulse components. In our calculations, we have considered $\alpha \geq 1$ and $\xi < 1$, which are in the parameter region formerly investigated in Ref. [48]. The envelope $f(t)$ (unless stated otherwise) is a squared-sine function,

$$f(t) = \begin{cases} V\sin(\pi t/T_w)^2 & \text{if } 0 \leq t \leq T_w, \\ 0 & \text{otherwise,} \end{cases} \tag{6}$$

where T_w is the pulse duration and V is the amplitude.

As in our previous works [49,50], we use the parameters of the OH bond in the water molecule, $D=5.42$ eV, $\beta^{-1}=0.445$ Å, $m=0.9482$ u, $r_e=0.9636$ Å, $q=1.634|e|$, and $r_d=0.6$ Å. In the following, we discuss the techniques used to solve the quantum and the classical equations of motion.

A. Quantum mechanics

The spectrum of the free Morse potential has a discrete and a continuous part. The discrete portion corresponds to the vibrational states with integer quantum numbers ν while the continuous sector represents the unbound states with real positive quantum numbers κ. The allowed bound energies are $E_\nu = -\hbar^2\beta^2(N-\nu)^2/2m$, where ν ranges from zero to the integer part of N, which is related to Morse parameters by $(N+1/2)^2 = 2mD/\hbar^2\beta^2$. For the parameters of the OH bond, $N \approx 21.58$ and the potential supports 22 vibrational levels. The energy in the continuous part is given by $E(\kappa) = \hbar^2\beta^2\kappa^2/2m$, where κ ranges from zero to infinity.

Numerical integration of the Schrödinger equation for the total Hamiltonian (1) was performed using a recently developed technique, which merges the standard basis-state approach with the expansion of the continuum coefficients in terms of generalized Laguerre polynomials [49,50]. The wave function can be written as

$$\Psi(r,t) = \sum_{\nu=0}^{\mathrm{int}(N)} a_\nu(t)\phi_\nu(r) + \int_0^\infty a(\kappa,t)\phi(\kappa,r)d\kappa, \tag{7}$$

where ϕ_ν and $\phi(\kappa)$ are, respectively, the discrete and continuum eigenfunctions.

Furthermore, the continuum coefficient $a(\kappa)$ can be expressed as

$$a(\kappa) = \sum_{n=0}^{\infty} \tilde{a}_n \mathcal{L}_n(\kappa), \tag{8}$$

where the functions $\mathcal{L}_n(\kappa)$ are related to the generalized Laguerre polynomials L_n^λ by

$$\mathcal{L}_n(\kappa) = N_n^\lambda k^{\lambda/2} e^{-\kappa\lambda/2} L_n^\lambda(\lambda\kappa), \tag{9}$$

where N_n^λ is a normalization constant and λ is an adjustable parameter (see Ref. [49] for details).

Substitution of the above expressions on the Schrödinger equation leads to a first-order system of ordinary differential equations for the coefficients a_ν and $\tilde{a}_n$ which can be solved by standard algorithms, such as Runge-Kutta. Analytical for-

mulas for the matrix elements that couples these equations can be found in Refs. [49,54]. This method provides accurate results while it is computationally simple to implement. Furthermore, it accounts for the continuum without the need of introducing artificial absorbing boundaries. We assume that the molecule has been previously prepared in some specific bound vibrational state ν and is then subject to the action of the laser pulse. The final dissociation probability, P_d, is defined by the total unbound population after the pulse, and correspondently can be calculated subtracting the total population of the bound states from one.

B. Classical mechanics

In order to compare the classical and quantum calculations, we must define a classical dissociation probability. A straightforward manner to do this is to propagate some large initial set of N_t trajectories in phase-space according to Hamilton's equations. Then one calculates the fraction of the escaping trajectories, $P_d=n/N_t$, for which the energy is greater than the dissociation energy by the end of the excitation. In our calculations, we have used $N_t=1000$, so that the classical dissociation probability was obtained to within a relative error less than 1% for the parameters considered here. Following the literature [37,44,46] we choose the ensemble of initial conditions on the energy shell of the corresponding vibrational quantum level. The canonical variables (r,p) of the unperturbed Hamiltonian (2) are conveniently written in terms of action-angle variables (I,θ) (see, for instance, Refs. [44,48]), and the N_t trajectories are uniformly distributed over the angle variable θ.

III. DISSOCIATION THRESHOLD DEPENDENCE ON THE PHASE

Initially, we analyze the effect of the relative phase ϕ of the two-color pulse, Eq. (5), on the dissociation probability of OH starting from the ground state. Figure 1 displays the quantum (solid lines) and the classical (dashed lines) dependence of the dissociation probability on the field amplitude, V, for pulses with duration of $T_w=0.5$ ps. The central pair of curves were obtained for one-color pulses, $\xi=0$, with carrier frequency $\omega=1000$ cm^{-1}. Note that although the classical and the quantum results do not agree for all values of the amplitude, the classical calculations still give a good estimate of the dissociation threshold. In particular, the value of the amplitude for which the quantum dissociation probability reaches 10% is 2.32 GV cm^{-1}, while the classical is 2.30 GV cm^{-1}. The remaining curves were obtained for $\xi=0.2$ and $\alpha=2$, corresponding to the addition of the second harmonic frequency. The leftmost curves were calculated with relative phase $\phi=\pi$ and the rightmost with $\phi=0$. This shows that the 10% dissociation threshold can be shifted by roughly 1 GV cm^{-1} by simply manipulating the relative phase between the components of the two-color pulse. Moreover, we see that both the quantum and the classical calculations show the same overall shift with the relative phase, which is a clear example of quantum-classical correspondence. It is worth noting that Fig. 1 is similar to the one

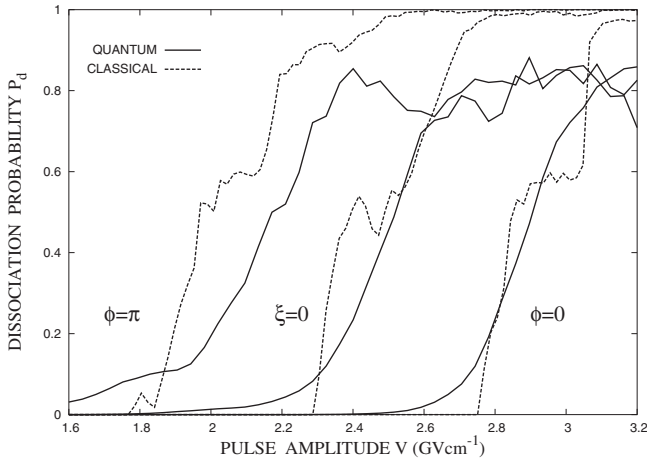

FIG. 1. Dissociation curves for OH in the $\nu=0$ state. Quantum (solid line) and classical (dashed line) probability versus excitation amplitude for pulse duration $T_w=0.5$ ps. One-frequency ($\xi=0$) results are for the frequency $\omega=1000$ cm^{-1} alone. Two-frequency ($\xi=0.2$) results are with a second harmonic added ($\alpha=2$), for relative phase $\phi=0$ (rightmost pair of curves) and $\phi=\pi$ (leftmost pair of curves).

previously obtained by Sirko and Koch [33] for the ionization of the hydrogen atom. However, here we considered ground-state molecules subject to infrared radiation in opposition of the highly excited states driven by microwave fields considered in Ref. [33]. In addition, as we discuss in the next section, the origin of the phase effect on the classical dissociation is related to deformations of regular KAM regions rather than to common resonances [48].

In order to establish the validity of the quantum-classical analogy of the phase shift in the dissociation curves, we studied the behavior of the dissociation threshold for several parameters of system. Starting with the OH in the ground state $\nu=0$ we consider pulses of different durations T_w and relative amplitude ratios ξ. In Fig. 2, we plot the dissociation threshold as a function of the relative phase ϕ. The pulses have frequency $\omega=500$ cm^{-1} and $\alpha=2$. The quantum results are represented by solid lines and classical by dashed lines. Panels (a) and (b) show the results for $T_w=0.25$ ps and $T_w=2$ ps, respectively, and the same amplitude ratio $\xi=0.25$. We note expressive shifts on the threshold, of about 1.5 GV cm^{-1}. In addition, the agreement between classical and quantum results is significantly better for the short pulse. For the longer pulse the classical calculations overestimate the quantum results by roughly 0.1 GV cm^{-1} for phases in the interval $[\pi/2:3\pi/2]$. This discrepancy, however, corresponds to less than 10% of the total variation of the threshold. Calculations with still longer pulses (up to $T_w=4$ ps) have yielded about the same result as in Fig. 2(b). Panels (c) and (d) were obtained for pulses with duration $T_w=1$ ps and amplitudes ratios $\xi=0.1$ and $\xi=0.55$, respectively. For $\xi=0.1$, the variation of the phase yields an overall shift of the threshold of about 0.5 GV cm^{-1}, which is considerably less than the shift of 1.1 GV cm^{-1} for $\xi=0.55$. Apart from small discrepancies, the quantum and classical results are very similar.

Another important aspect concerns the frequency ratio α between the pulse components. We show in Fig. 3 that the

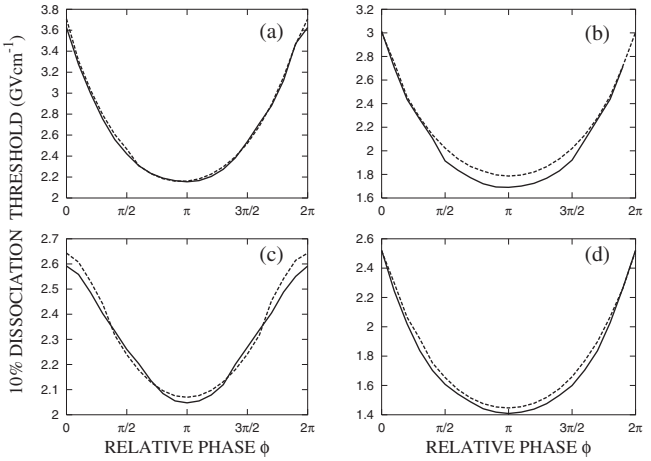

FIG. 2. The 10% dissociation threshold versus relative phase from the $\nu=0$ ground state. Quantum (solid line) and classical (dashed line) results for the frequency $\omega=500$ cm^{-1} and its second harmonic $\alpha=2$. (a) Pulse duration $T_w=0.25$ ps and relative component amplitudes $\xi=0.25$, (b) $T_w=2$ ps and $\xi=0.25$, (c) $T_w=1$ ps and $\xi=0.1$, (d) $T_w=1$ ps and $\xi=0.55$.

form of the threshold curve depends strongly on this parameter. Note that for $\alpha=1$, panel (a), and $\alpha=3$, panel (b), the curves have the opposite concavity as compared to the previous curves for $\alpha=2$, with the maximum of the threshold occurring for $\phi=\pi$ and minimum for $\phi=0$. It is also instructive to analyze the case of noncommensurate frequencies. For $\alpha=\pi/3$, panel (c), and $\alpha=2\pi/3$, panel (d), the curves are shifted, looking more sine-like, in contrast to the previous bell-shaped curves. By comparing panels (a) and (c), we verify that a small change in α can produce a large shift on the threshold curve, even though the overall variations of the threshold are roughly the same. Once again, good agreement is found between the classical and the quantum results.

The quantum-classical correspondence indicated by the 10% threshold plots is a reflection of the overall shift of the

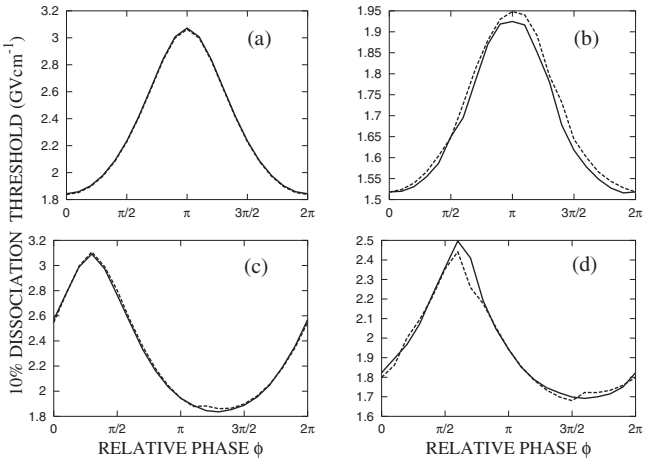

FIG. 3. Dissociation threshold from $\nu=0$ for distinct frequency ratios of the two-color pulses. Quantum (solid line) and classical (dashed line) results for $T_w=1$ ps and $\omega=500$ cm^{-1}. (a) Frequency ratio $\alpha=1$, amplitude ratio $\xi=0.25$. (b) $\alpha=3$, $\xi=0.4$. (c) $\alpha=\pi/3$, $\xi=0.25$. (d) $\alpha=2\pi/3$, $\xi=0.3$.

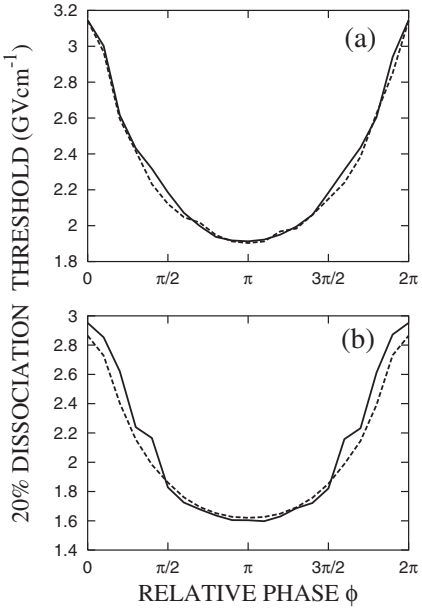

FIG. 4. The 20% dissociation threshold versus relative phase from the $\nu=0$ ground state. Quantum (solid line) and classical (dashed line) results for pulse duration $T_w=1$ ps, (a) amplitude ratio $\xi=0.2$, frequency $\omega=500$ cm^{-1}; (b) $\xi=0.3$, $\omega=1000$ cm^{-1} and their second harmonics $\alpha=2$.

dissociation probability curves as a function of the relative phase, as evidenced by Fig. 1. It is worth noting that the general agreement between the classical and quantum results do not display significant differences for other choices of the value to be considered as the outset of the molecule cleavage (at least for moderate dissociation probability $P_d<30\%$). For instance, panels (a) and (b) of Fig. 4 show the 20% threshold as a function of the relative phase for two-color fields with fundamental frequencies $\omega=500$ cm^{-1} and $\omega=1000$ cm^{-1} combined with their second harmonics, $\alpha=2$. It can be noted from both plots that the classical and quantum agreement persists, and that the 20% curves have similar shape compared to the 10% curves.

Finally, we turn our attention to the frequency ω of the pulse. Consider the resonance frequency between two vibrational levels ν and ν' given by $\omega_{\nu,\nu'}=|E_{\nu'}-E_{\nu}|/\hbar$. In Fig. 5, the dissociation threshold from the ground state is depicted for the external frequency ω equal to some fraction of the fundamental transition $\omega_{0,1}\approx 3784$ cm^{-1}. We note that as the frequency ω approaches the resonance condition to the first excited level, the quantum and classical results diverge. In panels (a) and (b), for which the external frequency is, respectively, $\omega_{0,1}/8$ and $\omega_{0,1}/4$, there is good agreement between the quantum and classical calculations. For the frequency $\omega=\omega_{0,1}/2$, panel (c), the second harmonic is already in resonance with the first excited level and the agreement deteriorates. For $\omega=\omega_{0,1}$, panel (d), the quantum-classical results are close only in a small interval of ϕ around π. The same qualitative behavior of the dissociation threshold was found for the system starting in excited states. Panels (a) and (b) of Fig. 6 show the threshold from $\nu=5$ for $\omega=\omega_{5,6}/8$ and $\omega=\omega_{5,6}\approx 2887$ cm^{-1} and panels (c) and (d) show the threshold from $\nu=10$ for $\omega=\omega_{10,11}/8$ and $\omega=\omega_{10,11}\approx 1989$ cm^{-1}.

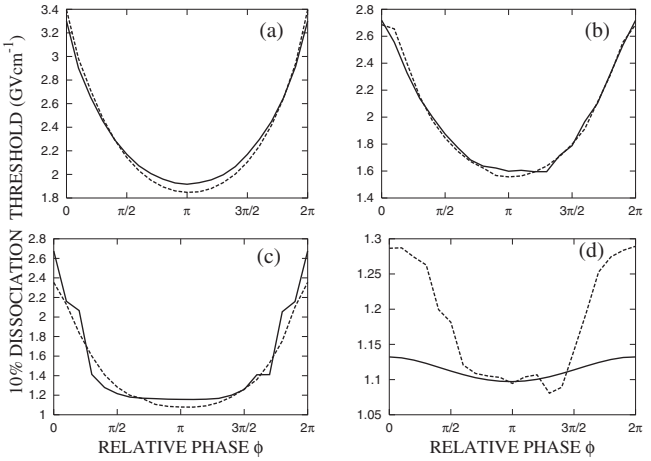

FIG. 5. Dissociation threshold from $\nu=0$ for pulses with distinct fundamental frequencies and their second harmonics. Quantum (solid line) and classical (dashed line) results for pulse duration $T_w=1$ ps, frequency ratio $\alpha=2$, and amplitude ratio $\xi=0.25$. (a) Frequency $\omega=\omega_{0,1}/8$. (b) $\omega=\omega_{0,1}/4$. (c) $\omega=\omega_{0,1}/2$. (d) $\omega=\omega_{0,1}$.

The agreement is noticeable in the cases (a) and (c), whereas the quantum and classical results in (b) and (d) are rather discrepant. It is clearly seen that the quantum-classical agreement is good for the off-resonance regime, whereas at the resonance frequency with the upper level, the results are divergent. Therefore, we conclude that the quantum and classical dependence of the threshold of dissociation on the phase agrees as long as the laser frequency is sufficiently far from the resonances with the quantum vibrational levels. For the parameters considered here, we verified very good quantum-classical correspondence for $\omega<\omega_{\nu,\nu'}/2$. This is evidence that classical mechanics is not able to reproduce the quantum results near resonances.

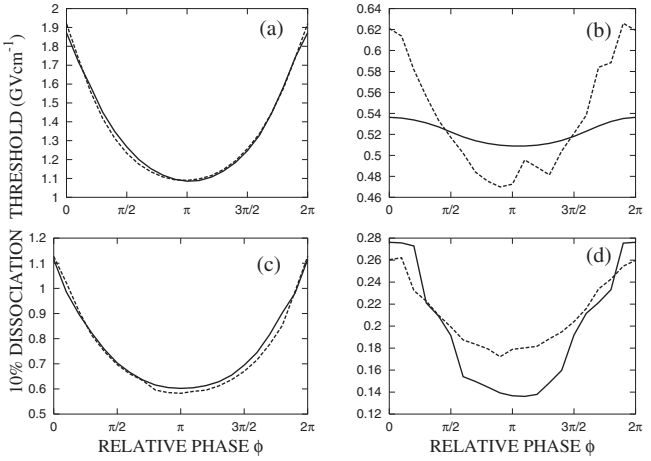

FIG. 6. Dissociation threshold from excited states for pulses with distinct fundamental frequencies and their second harmonics. Quantum (solid line) and classical (dashed line) results for pulse duration $T_w=1$ ps, frequency ratio $\alpha=2$, and amplitude ratio $\xi=0.25$. Initial state $\nu=5$: (a) Frequency $\omega=\omega_{5,6}/8$, (b) $\omega=\omega_{5,6}$. Initial state $\nu=10$: (c) $\omega=\omega_{10,11}/8$, (d) $\omega=\omega_{10,11}$.

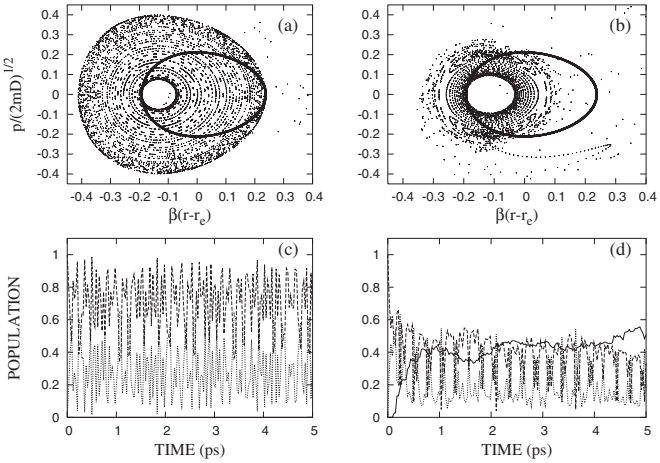

FIG. 7. Correspondence between the effects of the relative phase on the classical and quantum dynamics. The system is driven by squared pulses with duration $T_w=5$ ps, frequency $\omega=500$ cm^{-1}, amplitude 1.7 GV cm^{-1}, frequency ratio $\alpha=2$, and amplitude ratio $\xi=0.25$. The top panels show stroboscopic plots for (a) $\phi=0$ and (b) $\phi=\pi$ (in each panel, the closed bold curve represents the ensemble of initial conditions). The corresponding quantum population dynamics are shown in the bottom panels for the ground-state population (dashed curve), the remaining bound states (dotted curve) and the dissociation probability (solid curve) for (c) $\phi=0$ and (d) $\phi=\pi$.

IV. PHASE-SPACE STRUCTURE AND POPULATION DYNAMICS

In view of the results of the preceding section, it is enlightening to analyze the changes in the phase-space structure caused by the phase variation and its connection to the quantum dynamics. We consider a commensurate frequency ratio $\alpha=2$ and a squared envelope function $f(t)$,

$$f(t)=\begin{cases} V & \text{if } 0\le t\le T_w, \\ 0 & \text{otherwise,} \end{cases} \tag{10}$$

where T_w is the pulse duration and V is the amplitude.

The above parameters for the external field guarantee that the Hamiltonian is periodic in time, with period of $2\pi/\omega$, and the corresponding classical dynamics can be conveniently studied by stroboscopic plots [48]. The initial state is chosen to be the ground state and we fix the frequency $\omega=500$ cm^{-1}, the amplitude $V=1.7$ GV cm^{-1}, the amplitude ratio $\xi=0.25$, and the pulse duration $T_w=5$ ps. In Fig. 7, we depict stroboscopic maps along with the corresponding quantum population dynamics. The stroboscopic plot of panels (a) and (b) were obtained by recording the position and momentum of the initial set of trajectories (represented by the bold closed line) for each multiple of the time interval $2\pi/\omega$. In panel (a), the relative phase of the pulses is set to $\phi=0$ and we can see that the phase space is dominated by a KAM regular region. Most of the trajectories remain trapped in those regular orbits and the resulting dissociation probability is zero. The structural change in the phase space caused by the relative phase can be seen in panel (b), for which we adjusted the phase to $\phi=\pi$. The most conspicuous modifica-

tion is the shrinking of the region of KAM tori and the appearance of some resonance islands. As pointed out by Constatoudis and Nicolaides [48], those effects constitute the phase space origin of the relative phase effect on the dissociation probability. Out of the regular region, the trajectories lie in the chaotic sea and eventually escape from the potential well, leading to a dissociation probability of roughly 55.4%. The quantum companions of the stroboscopic plots are in panels (c) and (d), which show the dynamics of the ground-state population (dashed curves), the remaining bound population (dotted curves) and the dissociation probability (solid curve). In panel (c), we note that there is no dissociation, and we can see a strong oscillation between the ground state and the remaining bound states (noticeable population is found up to the third excited vibrational level). As in the classical case, the situation drastically changes with the alteration of the relative phase to $\phi=\pi$ shown in panel (d). The ground-state population suffers a sudden decrease, whereas the dissociation probability increases, reaching 50.7% by the end of the excitation. Therefore, it should be noted that the oscillation between the quantum levels for $\phi=0$ corresponds to the trapping of the classical trajectories in the regular orbits of phase space, whereas the quantum transition to the continuum leading to dissociation for $\phi=\pi$ have its classical correspondence with the trajectories lying in the chaotic sea due to the modifications in the phase-space structure induced by the relative phase. We also point out that similar analogies in the dissociation mechanisms were found for the excited states $\nu=5$ and $\nu=10$.

In order to shed some light on the lack of quantum-classical correspondence in the resonance regime, we now consider a field with frequency in resonance with the fundamental and first excited quantum levels, $\omega=\omega_{0,1}$. As before, the system is considered to be in the ground state and subjected to squared pulses with commensurate frequency ratio $\alpha=2$. The duration of the pulses is set to $T_w=1$ ps, the amplitude to $V=747.2$ MV cm^{-1}, while the amplitude ratio is $\xi=0.45$. The stroboscopic maps along with the corresponding quantum population dynamics are depicted in Fig. 8. In panel (a), the relative phase of the pulses is set to $\phi=0$. We can see several nonlinear resonance islands as well as some KAM tori around them. We also note a small part of the trajectories lying in the outermost chaotic region. However, none of these trajectories has enough time to escape from the well and the resulting dissociation probability is null. The change in the relative phase to $\phi=\pi$ cause the disappearance of most of the KAM tori and the growth and movement of the resonant islands, as displayed in panel (b). As a consequence, a significant number of trajectories lies in the chaotic sea and the final dissociation probability reaches 15.4%. The dynamics of the quantum populations subject to the same external fields are shown in panels (c) and (d) for $\phi=0$ and $\phi=\pi$, respectively. In both cases, there exists non-negligible probability of molecular breaking: $P_d=18.5\%$ for $\phi=0$ and $P_d=26.4\%$ for $\phi=\pi$. Although, like in the classical case, there is an increasing in the final dissociation probability caused by the change of the relative phase from zero to π, the quantum and classical results are rather discrepant. By comparing to the analogous panels of Fig. 7, it should be noted that the population dynamics of the excited states play

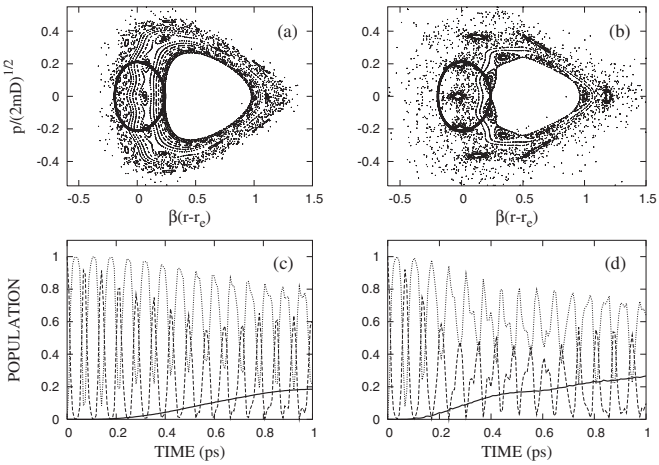

FIG. 8. Effects of the relative phase on the classical and quantum dynamics in the resonance regime. The system is driven by squared pulses with duration $T_w=1$ ps, frequency $\omega=\omega_{0,1}$, amplitude 747.2 MV cm^{-1}, frequency ratio $\alpha=2$, and amplitude ratio $\xi=0.45$. The top panels show stroboscopic plots for (a) $\phi=0$ and (b) $\phi=\pi$ (in each panel, the closed bold curve represents the ensemble of initial conditions). The corresponding quantum population dynamics are shown in the bottom panels for the ground-state population (dashed curve), the remaining bound states (dotted curve) and the dissociation probability (solid curve) for (c) $\phi=0$ and (d) $\phi=\pi$.

an important role in the dissociation process (see the dotted curves). That is, the excited bound levels acquire significant occupation probability during the action of the external pulse. This fact indicates that before reaching the continuum the system undergoes several multiphoton transitions. Indeed, we have found noticeable population ($>10\%$) up to the seventh excited level. These high-order transitions are expected since the resonance frequency $\omega_{0,1}$ is close to several multiphoton resonances and we are dealing with intense fields which enable nonlinear effects. For instance, the five-photon transition to the $\nu=5$ state is roughly $0.9\omega_{0,1}$. In addition, the second harmonic of the two-color field is almost in tune with the overtone transition from the ground to the second excited state and to the two-photon transition from the ground to the fourth excited level. Therefore, multiphoton transitions are paramount for the quantum dissociation mechanism. These transitions have an intrinsic quantum nature. They can be viewed as the result of constructive interferences between the phases associated with distinct paths. On the other hand, the classical calculations do not retain any phase information concerning the trajectories and the multiphoton transitions cannot be reproduced. Additional calculations have confirmed the same discrepancies in the quantum and classical results for the field frequency tuned to exact multiphoton resonances. Finally, it is important to note that the lack of agreement between quantum and classical energy absorption in the multiphoton resonance regime was observed in the seminal work of Walker and Preston [55] and also in the context of multiphoton dissociation in a more recent paper by Dimitriou *et al.* [41].

V. CONCLUSIONS

We have investigated the correspondence between the quantum and classical dynamics in the multiphoton dissociation of a diatomic molecule by two-color laser pulses. We have considered intense pulses (nonpertubative regime) of the order of picoseconds and the excitation from the ground state and also from excited levels. The main emphasis has been placed on the dependence of the dissociation threshold on the relative phase of the external field. We have also examined the classical phase space and the corresponding dynamics of the quantum populations in view of the change of the phase.

Our calculations show that both quantum and classical dissociation threshold can be controlled using the relative phase. We have investigated the threshold curves for several amplitude and frequency ratios between the components of the pulse. In analogy to the ionization of highly excited hydrogen atoms by two-color microwave fields [33], we have verified that the quantum and classical phase effects on the dissociation threshold of diatomic molecules by ultrashort (picoseconds) infrared laser pulses are in good agreement in the off-resonance regime. The examination of the classical stroboscopic plots along with the quantum dynamics reveals the connection between the phase-space structural modifications and the behavior of the quantum populations due to relative phase effects. We have shown that applying two-color pulses with frequency combined with its second harmonic, the oscillations between the quantum levels for zero relative phase corresponds to the trapping of most of the classical trajectories in the regular orbits of phase space, in which case there is no dissociation. On the other hand, for increasing phase the quantum transition to the continuum leading to dissociation have its classical correspondence with the trajectories lying in the chaotic sea that eventually escape from the potential well. Therefore, the shrinking of regular KAM regions in phase space is related to the increase of the quantum dissociation probability caused by the adjustment of the phase. This fact evidences the significance of the classical interpretation of the phase effects previously investigated by Constantoudis and Nicolaides [48]. However, it is important to point out, as we have also shown, that the quantum-classical correspondence breaks down when the laser frequency is tuned close to the multiphoton quantum resonances. This fact indicates that the energy absorption relative to the dissociation threshold of the quantum system in the resonance regime cannot be reproduced by the classical dynamics. The discrepancies between the quantum and classical results can be understood in view of the lost of phase information related to each trajectory by classical mechanics, as previously remarked by Walker and Preston [55].

The quantum-classical correspondence reported here highlights the relevance of classical calculations for the control of molecular systems, since it allows the interpretation of the phase effects on the dissociation threshold in terms of the changes in the classical phase-space structure, similar to those carried out in Refs. [33,48]. Finally, the present calculations encourage the investigation of this system using semiclassical theories, which should provide even better agreement with the exact quantum calculations and might bridge the gap between classical and quantum results in the resonance regime.

ACKNOWLEDGMENTS

This work was supported by Fundação de Amparo à Pesquisa do Estado de São Paulo (FAPESP) and CNPq, Brazil.

[1] I. Franco and P. Brumer, Phys. Rev. Lett. **97**, 040402 (2006).
[2] D. Jarukanont, K. Na, and L. E. Reichl, Phys. Rev. A **75**, 023403 (2007).
[3] S. Huang, C. Chandre, and T. Uzer, J. Phys. B **40**, F181 (2007).
[4] A. J. Makowski and K. J. Gorska, Phys. Lett. A **362**, 26 (2007).
[5] A. Kormanyos, Z. Kaufmann, J. Cserti, and C. J. Lambert, Phys. Rev. Lett. **96**, 237002 (2006).
[6] M. Kryvohuz and J. S. Cao, Phys. Rev. Lett. **95**, 180405 (2005).
[7] L. V. Vela-Arevalo and R. F. Fox, Phys. Rev. A **71**, 063403 (2005).
[8] G. Casati and B. Chirikov, *Quantum Chaos* (Cambridge University, Cambridge, 1995).
[9] F. Haake, *Quantum Signatures of Chaos* (Springer-Verlag, New York, 1992).
[10] L. E. Reichl, *The Transition to Chaos in Conservative Classical Systems: Quantum Manifestations* (Springer-Verlag, New York, 1992).
[11] M. Shapiro and P. Brumer, *Principles of the Quantum Control of Molecular Processes* (Wiley, New York, 2003).
[12] F. Ehlotzky, Phys. Rep. **345**, 175 (2001).
[13] R. J. Gordon and S. A. Rice, Annu. Rev. Phys. Chem. **48**, 601 (1997).
[14] G. K. Paramonov, Chem. Phys. **177**, 169 (1993).
[15] S. Shi and H. Rabitz, J. Chem. Phys. **92**, 364 (1990).
[16] R. Kosloff, S. A. Rice, P. Gaspard, S. Tersigni, and D. J. Tannor, Chem. Phys. **139**, 201 (1989).
[17] M. Shapiro, J. W. Hepbrun, and P. Brumer, Chem. Phys. Lett. **149**, 451 (1988).
[18] D. J. Tannor and S. A. Rice, J. Chem. Phys. **83**, 5013 (1985).
[19] S. Grafe, P. Marquetand, and V. Engel, J. Photochem. Photobiol., A **180**, 271 (2006).
[20] J. Gong and P. Brumer, Annu. Rev. Phys. Chem. **56**, 1 (2005).
[21] C. D. Schwieters and H. Rabitz, Phys. Rev. A **44**, 5224 (1991).
[22] V. A. Astapenko, Quantum Electron. **36**, 1131 (2006).
[23] H. Ohmura, N. Saito, and M. Tachiya, Phys. Rev. Lett. **96**, 173001 (2006).
[24] H. Ohmura, T. Nakanaga, and M. Tachiya, Phys. Rev. Lett. **92**, 113002 (2004).
[25] L. Sirko, S. A. Zelazny, and P. M. Koch, Phys. Rev. Lett. **87**, 043002 (2001).
[26] H. G. Muller, P. H. Bucksbaum, D. W. Schumacher, and A.

Zavriyev, J. Phys. B **23**, 2761 (1990).
[27] D. W. Schumacher, F. Weihe, H. G. Muller, and P. H. Bucksbaum, Phys. Rev. Lett. **73**, 1344 (1994).
[28] B. Sheehy, B. Walker, and L. F. DiMauro, Phys. Rev. Lett. **74**, 4799 (1995).
[29] H. M. Kim and R. Bersohn, J. Chem. Phys. **107**, 4546 (1997).
[30] E. E. Aubanel and A. D. Bandrauk, Chem. Phys. Lett. **229**, 169 (1994).
[31] H. Ohmura, F. Ito, and M. Tachiya, Phys. Rev. A **74**, 043410 (2006).
[32] K. J. Schafer and K. C. Kulander, Phys. Rev. A **45**, 8026 (1992).
[33] L. Sirko and P. M. Koch, Phys. Rev. Lett. **89**, 274101 (2002).
[34] V. Constantoudis and C. A. Nicolaides, Phys. Rev. E **64**, 056211 (2001).
[35] R. Graham and M. Hohnerbach, Phys. Rev. A **43**, 3966 (1991).
[36] D. Poppe and J. Korsch, Physica D **24**, 367 (1987).
[37] Y. Gu and J. M. Yuan, Phys. Rev. A **36**, 3788 (1987).
[38] R. M. O. Galvao, L. C. M. Miranda, and J. T. Mendonca, J. Phys. B **17**, L577 (1984).
[39] G. M. Zaslavsky, *The Physics of Chaos in Hamiltonian Systems* (Imperial College Press, London, 2007).
[40] A. J. Lichtenberg and M. A. Lieberman, *Regular and Chaotic Dynamics* (Springer-Verlag, New York, 1992).
[41] K. I. Dimitriou, V. Constantoudis, T. Mercouris, Y. Komninos, and C. A. Nicolaides, Phys. Rev. A **76**, 033406 (2007).
[42] A. Kenfack and J. M. Rost, J. Chem. Phys. **123**, 204322 (2005).
[43] J. H. Kim, W. K. Liu, and J. M. Yuan, J. Chem. Phys. **111**, 216 (1999).
[44] J. M. Yuan and W. K. Liu, Phys. Rev. A **57**, 1992 (1998).
[45] A. Guldberg and G. D. Billing, Chem. Phys. Lett. **186**, 229 (1991).
[46] M. E. Goggin and P. W. Milonni, Phys. Rev. A **37**, 796 (1988).
[47] R. Heather and H. Metiu, J. Chem. Phys. **88**, 5496 (1988).
[48] V. Constantoudis and C. A. Nicolaides, J. Chem. Phys. **122**, 084118 (2005).
[49] E. F. de Lima and J. E. M. Hornos, J. Chem. Phys. **125**, 164110 (2006).
[50] E. F. de Lima and J. E. M. Hornos, Chem. Phys. Lett. **433**, 48 (2006).
[51] M. D. Feit, J. R. Fleck, and A. Steiger, J. Comput. Phys. **47**, 412 (1982).
[52] C. Leforestier and R. E. Wyatt, J. Chem. Phys. **78**, 2334 (1983).
[53] M. V. Korolkov, J. Manz, and G. K. Paramonov, Chem. Phys. **217**, 341 (1997).
[54] E. F. de Lima and J. E. M. Hornos, J. Phys. B **38**, 815 (2005).
[55] R. B. Walker and R. K. Preston, J. Chem. Phys. **67**, 2017 (1977).